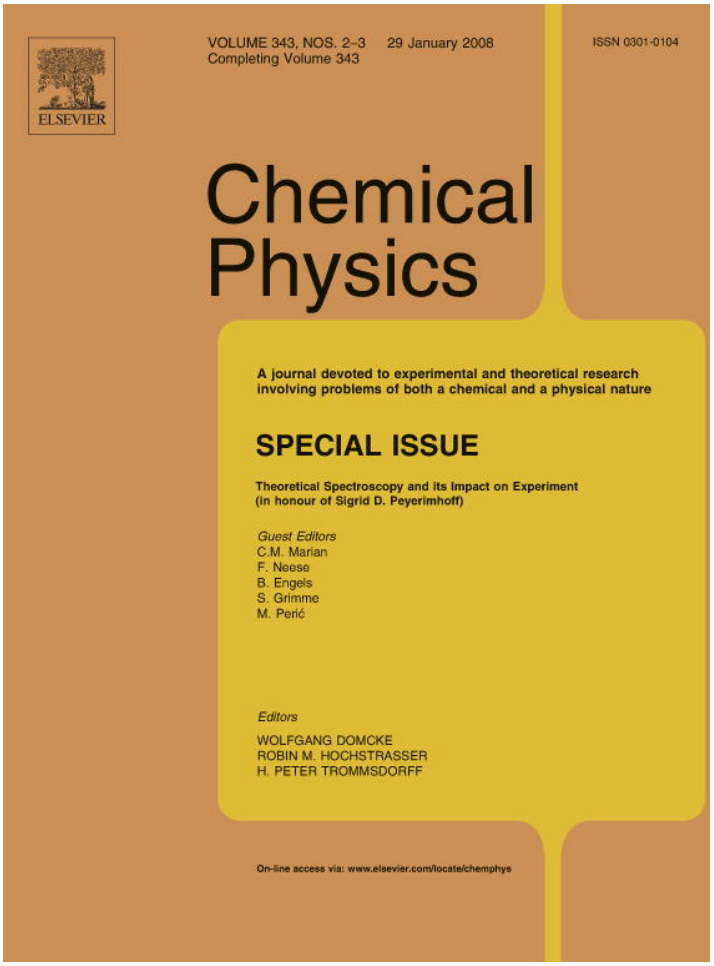

Available online at www.sciencedirect.com
ScienceDirect
Chemical Physics 343 (2008) 292–302
Chemical Physics
www.elsevier.com/locate/chemphys

Photodissociation of small carbonaceous molecules of astrophysical interest

M.C. van Hemert [a], E.F. van Dishoeck [b,*]

[a] Leiden Institute of Chemistry, Gorlaeus Laboratories, Leiden University, P.O. Box 9502, 2300 RA Leiden, The Netherlands
[b] Leiden Observatory, Leiden University, P.O. Box 9513, 2300 RA Leiden, The Netherlands

Received 4 June 2007; accepted 15 August 2007
Available online 22 August 2007

Abstract

Astronomical observations have shown that small carbonaceous molecules can persist in interstellar clouds exposed to intense ultraviolet radiation. Current astrochemical models lack quantitative information on photodissociation rates in order to interpret these data. We here present *ab initio* multi-reference configuration–interaction calculations of the vertical excitation energies, transition dipole moments and oscillator strengths for a number of astrophysically relevant molecules: C_3, C_4, C_2H, *l*- and *c*-C_3H, *l*- and *c*-C_3H_2, HC_3H, *l*-C_4H and *l*-C_5H. Highly excited states up to the 9th root of each symmetry are computed, and several new states with large oscillator strengths are found below the ionization potentials. These data are used to calculate upper limits on photodissociation rates in the unattenuated interstellar radiation field by assuming that all absorptions above the dissociation limit lead to dissociation.

PACS: 31.15.Ar; 31.50.Df; 33.15.Fm; 33.20; 33.70.Ca; 33.80.Gj; 95.30.Ky; 98.38.Bn; 98.38.–j

Keywords: Molecular data; Excited electronic states; Oscillator strengths; Photodissociation; Interstellar molecules

1. Introduction

Of the more than 130 different molecules found in interstellar space, an important class is formed by the unsaturated carbonaceous species. Carbohydrides ranging from small molecules such as C_2H [1] to long chains like C_8H [2] and $HC_{11}N$ [3] have been detected through their millimeter transitions in cold dark clouds like TMC-1 for several decades. Some of these molecules have also been seen in their cyclic form, with *c*-C_3H_2 as the best-known example [4]. Even negative ions, in particular C_6H^-, have now been detected [5]. Bare carbon chains are likely present as well but do not have a permanent dipole moment and can therefore not be observed through their pure rotational transitions in emission. Instead, the smallest members of this family, C_2 and C_3, have been detected in diffuse interstellar clouds, – i.e., clouds which are not completely opaque to visible and ultraviolet radiation – through their electronic absorptions against bright background stars [6–8]. *c*-C_3H_2 has been seen in diffuse clouds as well, through absorption at radio wavelengths against background quasars [9]. The relatively large abundances of these non-saturated molecules, in spite of the fact that there is 10^4 times more hydrogen than carbon in interstellar clouds, are a vivid demonstration that interstellar chemistry is not in thermodynamic equilibrium. Instead, the kinetics of the reactions that form and destroy these molecules need to be taken into account explicitly in order to explain their abundances. In cold dark clouds, these traditionally involve a series of ion–molecule and neutral–neutral reactions [10,11].

More recently, several of the carbohydrides C_nH_m have also been observed in so-called photon-dominated regions (PDRs) [12], i.e., clouds which are exposed to intense ultraviolet (UV) radiation. Species like C_2H and *c*-C_3H_2

* Corresponding author.
E-mail address: ewine@strw.leidenuniv.nl (E.F. van Dishoeck).

0301-0104/$ - see front matter © 2007 Elsevier B.V. All rights reserved.
doi:10.1016/j.chemphys.2007.08.011

have been detected in the Orion Bar PDR [13] and even more complex molecules like C_3H_2 and C_4H have been seen in the Horsehead nebula, M38 [14,15]. Together with the above mentioned observations of diffuse clouds, the data demonstrate that these molecules can exist in UV-exposed environments with abundances comparable to those in cold dark clouds. Traditional PDR chemical models cannot explain the high abundances of these molecules, leading to speculations that they are perhaps produced by fragmentation of even larger carbonaceous molecules such as polycyclic aromatic hydrocarbons (PAHs) [15]. However, a major uncertainty in these and other models are the photodissociation rates of the carbohydrides, which are basically unknown.

Other regions in which ultraviolet photons play a role in the chemistry include the envelopes of evolved stars and cometary atmospheres. The same carbohydride molecules have been detected in the envelope of the carbon-rich late-type star IRC + 10216, where their similar distributions are a puzzle for photochemical models [16]. In cometary atmospheres, species as complex as C_4H have been inferred, whose presence is not readily explained by the standard parent–daughter photochemical models [17].

Many theoretical studies of the electronic structure of small carbohydride molecules exist in the literature (e.g., [18–23]). However, most of them are limited to the ground and lowest few excited electronic states. Only few studies of higher states exist, most of them performed by Peyerimhoff and her co-workers starting more than 30 years ago, e.g., [24,25]. As will be shown here, those results are still highly relevant and provide an excellent starting point for further studies.

The aim of this paper is to provide insight into the photodissociation processes of carbohydride molecules through *ab initio* quantum chemical calculations of the vertical excitation energies and oscillator strengths for as large a number of excited electronic states as feasible with current programs. By assuming that most of the absorptions with energies above the dissociation limit lead to destruction, estimates of the (upper limits of) photodissociation rates under interstellar conditions can be obtained. Even though such calculations are necessarily limited to the smaller members of the carbohydride family, they do provide quantitative constraints to test the basic interstellar chemical networks. Specifically, C_2H, C_3, C_4, *l*- and *c*-C_3H, *l*- and *c*-C_3H_2, HC_3H, *l*-C_4H and *l*-C_5H are studied here. Except for HC_3H, all these species have been chosen to have been observed in interstellar space.

2. Methods

2.1. Electronic structure calculations

For small diatomic and triatomic molecules, quantum chemical calculations of the potential energy surfaces and transition dipole moments combined with dynamical calculations of the nuclear motions can provide photodissociation cross sections and oscillator strengths that agree with experiments to better than 20–30%, e.g., [26–28] (see [29] for an early review). For the polyatomic molecules considered here, calculations of the full potential surfaces including all degrees of freedom become very time consuming, as do the multi-dimensional dynamics. Moreover, such detail is not needed in order to compute photorates, since those are largely determined by the potentials and transition moments in the Franck–Condon region. The simplest alternative is therefore to only compute the vertical excitation energies and transition dipole moment of the molecule at its equilibrium position and assume a certain probability that absorption into each excited state above the dissociation limit leads to dissociation. For the examples cited above, such an approach leads to similar rates within the accuracy of the calculations. The focus of our calculations is therefore on electric dipole-allowed transitions to states lying above the lowest dissociation limit but below 13.6 eV. The interstellar radiation field has a broad spectrum from visible to extreme ultraviolet wavelengths, peaking in intensity around 7 eV and cutting off at the atomic H ionization potential at 13.6 eV [30].

All calculations presented here were performed with the Wuppertal–Bonn MRDCI set of programs as implemented in the GAMESS-UK program package version 7.0 [31]. For C, the TZVP atomic orbital basis set was used, and for H, the DZP basis set [32]. To allow for a proper description of molecular Rydberg states, two diffuse p and two diffuse d functions were put on specific sites. For C_2 and C_2H, this was the middle of the CC bond; for C_2 and C_4H the middle of the C1–C2 and C3–C4 bonds; for C_3, *l*-C_3H, *l*-C_3H_2 and HC_3H the middle C; for C_5 on C2 and C4; for *c*-C_3H on the C connected to H; and for *c*-C_3H_2 on the lone C. These sites were chosen to avoid linear dependencies in the atomic orbital basis set due to large overlap of diffuse functions positioned on adjacent atoms. Cartesian d functions were used, of which the spherical component served as the 3s basis function.

Molecular orbitals were generated using up to the maximum number of reference states, 255. The selection threshold was generally set at 0.5 μhartree. The total number of configurations included in the configuration interaction (CI) calculation ranged from 200,000–400,000 per symmetry. The sum over the coefficients-squared in the final CI wave function is typically 0.95 for the smaller species, dropping to 0.9 for the larger molecules. The CI energies were extrapolated and corrected using the Davidson extrapolation [33]. The aim was to compute as many excited electronic states as feasible, up to 9 per symmetry. For the lower states, comparison with existing calculations and experiments indicates accuracies within 0.3 eV, generally better. Oscillator strengths to the lower states agree within 30% or better. For the higher states, typically the 5th root and higher per symmetry, the accuracy decreases because many states and orbitals can mix. Nevertheless, such calculations should still provide insight into the location of those states, in particular whether they are above or below the

ionization potential and below the 13.6 eV cutoff of the interstellar radiation field. Moreover, the magnitude of the oscillator strengths (strong or weak) should be reliable. Note that the precise values of the excitation energies are not so important for the purposes of calculating interstellar photorates because of the broad range of incident energies. The only exception is possible overlap with Lyman α radiation at 10.2 eV, which is important for certain astrophysical environments [34].

In all calculations, the largest Abelian subgroup of the full $C_{\infty v}$ group, C_{2v}, was used, with the molecule put along the z-axis. The doubly degenerate states are then split into the B_1 and B_2 irreducible representations for Π and Φ states, and into A_1 and A_2 for the Δ states. In general, the degeneracies for the Δ states are recovered within a few hundreds of an eV in the calculations. The average of the two A_1 and A_2 values is tabulated here. The A_1 irreducible representation also contains the Σ^+ states, and the A_2 the Σ^- states. Some excited states with electronic angular momentum higher than 2 (in particular Φ states) are also found in our calculations but they are not tabulated here since the electric dipole transition moments from the ground state to these states are zero, implying that they do not contribute to photodissociation. The valence or Rydberg character of the states is determined from calculations of the x^2, y^2 and z^2 expectation values.

Calculations have been limited to the equilibrium geometry corresponding to the lowest energy. For C_3, C_2H, C_4, C_4H and C_5H this is the linear geometry. C_3H and C_3H_2 have been detected in various isomeric forms so both cyclic and (near-)linear forms have been studied.

The dissociation energies for C_nH are calculated as the difference between the ground state energy of C_nH at its equilibrium geometry and the energy of ground state C_n, also at its equilibrium geometry, calculated in the presence of an H atom positioned at a distance of 20 Bohr from the center of mass. In this way the errors associated with the lack of size consistency are significantly reduced. Note that the spatial symmetry of the molecule and the fragment generally differs.

2.2. Photodissociation rates

Oscillator strengths to all excited states have been calculated according to

$$f_{\mathrm{ul}}^{\mathrm{el}} = \frac{2}{3}\, g_{\mathrm{ul}} \Delta E_{\mathrm{ul}}\, \mu_{\mathrm{ul}}^2 \tag{1}$$

where all quantities are in atomic units (a.u.), μ_{ul} is the transition dipole moment from lower state l to upper state u, and g_{ul} is a degeneracy factor which is 2 for a $\Pi \leftarrow \Sigma$ transitions and 1 for any other transition. For linear molecules, the dipole moment operator contained in μ_{ul} corresponds to $-\sum z_j$ for transitions between states with the same value of the electronic angular momentum projection quantum number Λ and to $-\sum(x_j + \mathrm{i}y_j)/\sqrt{2}$ for transitions with $\Delta\Lambda = \pm 1$. The computed excitation energies ΔE_{ul} were used in this formula, not any experimental values. Hence, differences with other work can stem from differences in both μ_{ul} and in ΔE_{ul}.

The photodissociation rate of a molecule can be computed from

$$k_{\mathrm{pd}}^{\mathrm{cont}} = \int \sigma(\lambda) I(\lambda)\, \mathrm{d}\lambda \quad \mathrm{s}^{-1} \tag{2}$$

where σ is the photodissociation cross section in cm^2 and I is the mean intensity of the radiation in photons $\mathrm{cm}^{-2}\,\mathrm{s}^{-1}\,\text{Å}^{-1}$ [34]. Under interstellar conditions, only single-photon processes are important. For photodissociation initiated by line absorptions (e.g., predissociation), the rate becomes

$$k_{\mathrm{pd}}^{\mathrm{line}} = \frac{\pi e^2}{mc^2} \lambda_{\mathrm{ul}}^2 f_{\mathrm{ul}} \eta_{\mathrm{u}} I_{\mathrm{ul}} \quad \mathrm{s}^{-1} \tag{3}$$

where η_{u} the dissociation efficiency of state u, which lies between 0 and 1. The numerical value of the factor $\pi e^2/mc^2$ is 8.85×10^{-21} in the adopted units with λ in Å. The total photodissociation rate of a molecule is obtained by summing over all channels. In this work, no dynamical calculations are performed to obtain continuous cross sections for dissociative states. Hence, all photorates are computed with Eq. (3). It is furthermore assumed that the dissociation efficiency $\eta_{\mathrm{u}} = 1$, either through direct dissociation in a repulsive state or by predissociation. The motivation for this choice is that for larger molecules, internal conversion to a lower (dissociative) electronic state is usually much more rapid than any radiative decay rates owing to the high density of states [35]. Specific experimental evidence of high dissociation efficiencies will be presented in the results section for individual molecules.

3. Results

3.1. C_2H

The C_2H radical, detected in interstellar clouds since 1974 [1], is an important step in the formation of longer carbon chains. In comets, it could be a photodissociation product of C_2H_2 and a precursor of the widely observed C_2 molecule. Given also its importance in combustion processes, this radical has received ample theoretical attention, starting with the papers by Shih, Peyerimhoff and co-workers [24,36] and culminating with the more recent two-dimensional potential surfaces by Duflot et al. [37].

As a test of our computational procedure, we present in Table 1 our computed vertical excitation energies, oscillator strengths and the main configurations of each state. Our energies generally agree well within 0.3 eV with those of Koures and Harding [38] (their CI + DV2 results) and lie in between those of Duflot et al. [37] and Shih et al. [24]. Close inspection shows that the larger differences are usually for states with Rydberg character (which are not included in Duflot et al. [37]) or for states with a strong interaction with a neighboring state, leading sometimes even to a switch in the character of the state. For example,

Table 1
Vertical excitation energies, oscillator strengths and dominant configurations for C_2H at the ground state equilibrium geometry

State	Energy (eV)				f^{el}	Dominant configuration	Type[a]
	This work	Ref. [38]	Ref. [37]	Ref. [24]	This work		
$1^2\Sigma^{+b}$	0.00	0.00	0.00	0.00	...	$\cdots 4\sigma^2 5\sigma^1 1\pi^4$	V
$2^2\Sigma^+$	7.06	6.73	6.63	7.32	4.0(−4)[c]	$\cdots 4\sigma^2 5\sigma^1 1\pi^3 2\pi^1$	V
$3^2\Sigma^+$	8.63	8.11	8.19	9.60	4.0(−5)	$\cdots 4\sigma^1 5\sigma^2 1\pi^4$	V
$4^2\Sigma^+$	9.28	9.01	9.21	9.18	3.0(−3)	$\cdots 4\sigma^2 5\sigma^1 1\pi^3 3px^1$	R
$5^2\Sigma^+$	10.09	10.09			2.8(−1)	$\cdots 4\sigma^2 5\sigma^1 1\pi^3 4px^1$	R
$6^2\Sigma^+$	10.28				1.0(−5)	$\cdots 4\sigma^2 5\sigma^1 1\pi^3 3px^1$	R
$1^2\Pi$	0.68	0.60	0.54	0.96	1.7(−3)	$\cdots 4\sigma^2 5\sigma^2 1\pi^3$	V
$2^2\Pi$	7.63	7.29	7.07	8.11	1.0(−2)	$\cdots 4\sigma^2 5\sigma^2 1\pi^2 2\pi^1$	V
$3^2\Pi$	8.39	8.17	8.05	9.96	1.0(−1)	$\cdots 4\sigma^2 5\sigma^1 1\pi^3 3s^1$	R
$4^2\Pi$	9.00	8.68	8.34	8.48	3.0(−2)	$\cdots 4\sigma^2 5\sigma^1 1\pi^3 3pz^1$	R
$5^2\Pi$	9.47		8.70		3.0(−2)	$\cdots 4\sigma^2 5\sigma^1 1\pi^3 3s^1$	R
$6^2\Pi$	9.96		8.80	9.22	2.2(−2)	$\cdots 4\sigma^2 5\sigma^1 1\pi^3 4pz^1$	R
$7^2\Pi$	10.06		9.25	9.78	1.1(−2)	$\cdots 4\sigma^2 5\sigma^1 1\pi^3 3pz^1$	R
$8^2\Pi$	10.33		9.67	10.40	4.6(−2)	$\cdots 4\sigma^2 5\sigma^1 6\sigma^1 1\pi^3$	M
$1^2\Sigma^-$	7.61	7.48	7.34	8.13		$\cdots 4\sigma^2 5\sigma^1 1\pi^3 2\pi^1$	V
$2^2\Sigma^-$	8.90	8.97	9.31	9.13		$\cdots 4\sigma^2 5\sigma^1 1\pi^3 2\pi^1$	V
$3^2\Sigma^-$	9.30					$\cdots 4\sigma^1 5\sigma^2 1\pi^3 3px^1$	R
$4^2\Sigma^-$	10.32					$\cdots 4\sigma^2 5\sigma^1 1\pi^3 3px^1$	R
$5^2\Sigma^-$	10.46					$\cdots 4\sigma^2 5\sigma^1 1\pi^3 3px^1$	R
$6^2\Sigma^-$	10.69					$\cdots 4\sigma^2 5\sigma^1 1\pi^3 3px^1$	R
$1^2\Delta$	7.89	7.70	7.57	8.27		$\cdots 4\sigma^2 5\sigma^1 1\pi^3 2\pi^1$	V
$2^2\Delta$	8.25	8.12	7.95	8.81		$\cdots 4\sigma^2 5\sigma^1 1\pi^3 2\pi^1$	V
$3^2\Delta$	9.20	9.06	9.23	9.12		$\cdots 4\sigma^{\sigma^2} 5\sigma^1 1\pi^3 3px^1$	R

[a] V = Valence; R = Rydberg; M = mixed in this and subsequent tables.
[b] Ground state energy including Davidson correction: −76.432130 hartree.
[c] Notation $x(-y)$ in this and subsequent tables indicates $x \times 10^{-y}$.

the $4^2\Sigma^+$ state in our calculation has Rydberg $3p_\pi$ character whereas it has ... $4\sigma^1 1\pi^3 5\sigma^2 3\pi^1$ in Duflot et al., resulting also in a very different transition dipole moment (see below).

Our computed $A^2\Pi$–$X^2\Sigma^+$ transition dipole moment of 0.22 a.u. is very close to that of 0.23 a.u. computed by Duflot et al. [37] and Peric et al. [39]. Because of the slightly higher excitation energy in our work, the oscillator strengths show somewhat larger differences. Comparison for other states is difficult since Duflot et al. do not give any numerical values. However, their Fig. 7 shows that neither the 3 and $4^2\Sigma^+$, nor the 2 and 3 $^2\Pi$ states have significant transition dipole moment. This is generally consistent with our results. For the $5^2\Sigma^+$ state we find a huge transition dipole moment of 1.1 a.u. due to the Rydberg character of our wavefunction. Thus, this state around 10 eV will dominate the interstellar C_2H photodissociation but the higher $^2\Pi$ states in the 8.5–10.5 eV range can also contribute significantly up to the ionization potential of ~11.4 eV (Table 11).

3.2. C_3

The C_3 molecule was detected in cometary spectra in 1882 through its A–X system at 4050 Å [40] and in interstellar clouds more than a century later [41,8]. The molecule is also seen in the atmospheres of cool carbon stars through its mid-infrared [42] and far-infrared [43] transitions (see [23] for review).

C_3 is a linear molecule with a ground $X^1\Sigma_g^+$ state. Its dissociation energy is computed to be about 4.6 eV, whereas its ionization energy is around 12 eV (Table 11). Quantum chemical studies range from the early work by Chabalowski et al. [44] to the recent calculations by Terentyev et al. [45]. Table 2 summarizes our computed excitation energies, together with the oscillator strengths and main configurations. For the low-lying valence states, our results agree to better than 0.3 eV with the MR-AQCC values of Monninger et al. [46]. These results also show that the $^1\Sigma_u^+ \leftarrow X^1\Sigma_g^+$ ($1\pi_u \rightarrow 1\pi_g$) transition at 8.17 eV has by far the largest oscillator strength, as predicted first by Pitzer and Clementi [47]. This is confirmed by the combined experimental and theoretical study by Monninger et al. [46] whose 1100–5600 Å spectrum demonstrates that the $^1\Sigma_u^+ \leftarrow X^1\Sigma_g^+$ transition around 1700 Å is indeed the strongest band. Their experiments in Ne and Ar matrices show a broad band but with some progressions superposed, which are evidence for interstate vibronic coupling with adjacent Π_g states. Indeed, the $^1\Sigma_u^+$ state is predicted to be unstable to bending, leading to avoided crossings with the lower-lying Π_g states [46]. These interactions can also lead to dissociative channels to produce $C_2 + C$.

3.3. C_3H

Both linear and cyclic C_3H have been detected in the interstellar medium by their transitions at millimeter wavelengths [48,49]. The $^2\Pi$ ground state of *l*-C_3H lies about

Table 2
Vertical excitation energies, oscillator strengths and dominant configurations for C_3 at the ground state equilibrium geometry

State	Energy (eV)		f^{el}	Dominant configuration	Type
	This work	Ref. [46]	This work		
$1^1\Sigma_g^{+a}$	0.00	0.00	···	$\cdots 4\sigma_g^2 3\sigma_u^2 1\pi_u^4$	V
$2^1\Sigma_g^+$	5.87			$\cdots 3\sigma_u^2 1\pi_u^4 1\pi_g^2$	V
$3^1\Sigma_g^+$	8.47			$\cdots 4\sigma_g^2 3\sigma_u^2 1\pi_u^2 1\pi_g^2$	V
$1^1\Sigma_u^+$	8.17	7.97	1.1(+0)	$\cdots 4\sigma_g^2 3\sigma_u^2 1\pi_u^3 1\pi_g^1$	V
$1^1\Pi_u$	3.21	3.11	5.0(−2)	$\cdots 4\sigma_g^2 3\sigma_u^1 1\pi_u^4 1\pi_g^1$	V
$2^1\Pi_u$	8.12	7.71	7.0(−4)	$\cdots 4\sigma_g^1 3\sigma_u^2 1\pi_u^3 1\pi_g^2$	V
$3^1\Pi_u$	8.64		7.2(−5)	$\cdots 4\sigma_g^1 3\sigma_u^2 1\pi_u^3 1\pi_g^2$	V
$4^1\Pi_u$	10.13		2.0(−1)	$\cdots 4\sigma_g^2 3\sigma_u^2 1\pi_u^3 3s$	R
$1^1\Pi_g$	4.01	4.00		$\cdots 4\sigma_g^1 3\sigma_u^2 1\pi_u^4 1\pi_g^1$	V
$2^1\Pi_g$	7.31	7.20		$\cdots 4\sigma_g^2 3\sigma_u^1 1\pi_u^3 1\pi_g^2$	V
$3^1\Pi_g$	7.46	7.89		$\cdots 4\sigma_g^2 3\sigma_u^1 1\pi_u^3 1\pi_g^2$	V
$4^1\Pi_g$	8.10			$\cdots 4\sigma_g^2 3\sigma_u^1 1\pi_u^3 1\pi_g^2$	V
$5^1\Pi_g$	8.86			$\cdots 4\sigma_g^2 3\sigma_u^1 1\pi_u^3 1\pi_g^2$	V
$1^1\Sigma_u^-$	4.29	3.98		$\cdots 4\sigma_g^2 3\sigma_u^2 1\pi_u^3 1\pi_g^1$	V
$2^1\Sigma_u^-$	6.20			$\cdots 4\sigma_g^1 3\sigma_u^1 1\pi_u^4 1\pi_g^2$	V
$1^1\Delta_g$	5.18			$\cdots 4\sigma_g^2 1\pi_u^4 1\pi_g^2$	V
$2^1\Delta_g$	9.45			$\cdots 4\sigma_g^2 3\sigma_u^2 1\pi_u^2 1\pi_g^2$	V
$3^1\Delta_g$	9.78			$\cdots 4\sigma_g^2 3\sigma_u^2 1\pi_u^3 2\pi_u^1$	V
$4^1\Delta_g$	9.95			$\cdots 3\sigma_u^2 1\pi_u^4 1\pi_g^2$	V
$1^1\Delta_u$	4.36	4.02		$\cdots 4\sigma_g^2 3\sigma_u^2 1\pi_u^3 1\pi_g^1$	V

[a] Ground state energy including Davidson correction: −113.735304 hartree.

Table 3
Vertical excitation energies, oscillator strengths and dominant configurations for l-C_3H at the ground state equilibrium geometry

State	Energy (eV)		f^{el}	Dominant configuration	Type
	This work	Ref. [51]	This work		
$1^2\Pi^a$	0.00	0.00	···	$\cdots 7\sigma^2 1\pi^4 2\pi^1$	V
$2^2\Pi$	3.69	3.92	2.9(−4)	$\cdots 7\sigma^2 1\pi^3 2\pi^2$	V
$3^2\Pi$	4.99	5.33	1.4(−3)	$\cdots 7\sigma^2 1\pi^3 2\pi^2$	V
$4^2\Pi$	5.39		7.4(−3)	$\cdots 7\sigma^2 1\pi^3 2\pi^2$	V
$5^2\Pi$	6.51		6.6(−2)	$\cdots 7\sigma^2 1\pi^4 3p_\pi^1$	R
$6^2\Pi$	7.56		2.9(−2)	$\cdots 7\sigma^1 1\pi^4 2\pi^1 3s$	R
$7^2\Pi$	7.82		3.5(−2)	$\cdots 7\sigma^2 1\pi^4 3p_\pi^1$	R
$8^2\Pi$	7.87		1.3(−1)	$\cdots 7\sigma^2 1\pi^4 3p_\pi^1$	R
$1^2\Sigma^+$	3.45	3.66	7.0(−3)	$\cdots 7\sigma^1 1\pi^4 2\pi^2$	V
$2^2\Sigma^+$	5.53		5.2(−4)	$\cdots 7\sigma^2 1\pi^4 3s^1$	R
$3^2\Sigma^+$	6.62		1.5(−2)	$\cdots 7\sigma^2 1\pi^4 3p_\sigma^1$	R
$4^2\Sigma^+$	7.30		1.7(−3)	$\cdots 7\sigma^1 1\pi^3 2\pi^3$	V
$5^2\Sigma^+$	8.15		2.2(−2)	$\cdots 7\sigma^2 1\pi^4 4p_\sigma^1$	R
$1^2\Sigma^-$	3.10	3.08	8.8(−3)	$\cdots 7\sigma^1 1\pi^4 2\pi^2$	V
$2^2\Sigma^-$	5.67		3.5(−3)	$\cdots 7\sigma^1 1\pi^3 2\pi^3$	V
$3^2\Sigma^-$	7.15		5.2(−3)	$\cdots 7\sigma^1 1\pi^3 2\pi^3$	V
$4^2\Sigma^-$	8.03		1.1(−2)	$\cdots 7\sigma^1 1\pi^4 3\pi^2$	R
$5^2\Sigma^-$	8.71		3.8(−3)	$\cdots 7\sigma^1 1\pi^4 2\pi^1 3p_\pi^1$	R
$1^2\Delta$	2.79	2.96	7.6(−3)	$\cdots 7\sigma^1 1\pi^4 2\pi^2$	V
$2^2\Delta$	6.86		4.0(−3)	$\cdots 7\sigma^1 1\pi^3 2\pi^3$	V
$3^2\Delta$	7.63		2.6(−3)	$\cdots 7\sigma^1 1\pi^3 2\pi^3$	V
$4^2\Delta$	8.24		5.8(−3)	$\cdots 7\sigma^1 1\pi^4 3\pi^2$	R

[a] Ground state energy including Davidson correction: −114.381395 hartree.

0.4–0.6 eV above the $^2B_2$ ground state of c-C_3H [50], with a small barrier toward the cyclic state. Hence, when C_3H is produced in its linear form by some sequence of ion molecule or other chemical processes, it can be stable, and both isomers are therefore considered in this work.

3.3.1. l-C_3H

The geometry of the $1^2\Pi$ state was taken from the experimental work of McCarthy and Thaddeus [69]. Table 3 summarizes our computed vertical excitation energies, oscillator strengths, and the corresponding configurations. Comparison with the CASSCF results of Ding et al. [51] shows good agreement for the lowest states. The dissociation energy of l-C_3H to $C_3 + H$ is computed at 3.3 eV. Of the dipole-allowed states above this dissociation limit, the higher $^2\Pi$ states around 7.8 eV have the largest oscillator strengths, in particular the $8^2\Pi$ state, which will dominate the photodissociation of the molecule.

3.3.2. c-C_3H

The c-C_3H radical has C_{2v} geometry in its 1^2B_2 ground state, with the equilibrium structure for our calculations taken from Yamamoto and Saito [52]. Table 4 summarizes our computed vertical excitation energies, oscillator strengths and configurations. Comparison with the CASSCF results of Ding et al. [51] shows again good agreement for the lowest states to 0.1–0.2 eV. The dissociation energy of c-C_3H to $C_3 + H$ is around 4.3 eV whereas its ionization potential is computed to lie at 9.6 eV (Table 11). Of the dipole-allowed states above the dissociation limit, the 2^2A_1 state around 5 eV and the higher $^2A_2$ states around 7.5 eV have the largest oscillator strengths, but the sum over the other states is comparable. Thus, there appear to be many potential routes to photodissociation for c-C_3H.

3.4. C_3H_2

Cyclopropenylidene, c-C_3H_2, was the first cyclic molecule to be detected in the interstellar medium [4] and subsequently found to be ubiquitous throughout the Galaxy, even in diffuse gas [53,9]. The near-linear form HCCCH (propargylene), denoted here as HC_3H, lies 0.4–0.8 eV higher in energy [54,50], depending whether the zero-point vibrational energy is included. Since it has a near-zero dipole moment, it has not yet been observed in interstellar clouds through radio transitions but is likely present as well. There are various other stable isomers of C_3H_2, of which another linear form, H_2CCC (vinylidenecarbene or propadienylidene), denoted here as l-C_3H_2, was discovered in interstellar space in 1991 [55]. It lies ~0.6 eV above the cyclic ground state including zero-point vibrational energy corrections [54]. Hence, all three isomers are considered in this work. Although there are many theoretical studies of the ground states of the various C_3H_2 isomers dating back to 1976 [56,18,57], the excited states are largely unexplored.

Table 4
Vertical excitation energies, oscillator strengths and dominant configurations for c-C_3H at the ground state equilibrium geometry

State	Energy (eV)		f^{el}	Dominant configuration	Type
	This work	Ref. [51]	This work		
1^2B_2[a]	0.00	0.00	⋯	$\cdots 5a_1^2 6a_1^2 1b_1^2 2b_2^2 3b_2^1$	V
2^2B_2	6.79	6.62	4.0(−3)	$2b_2 \rightarrow 3b_2$	V
3^2B_2	6.94		6.4(−3)	$6a_1 \rightarrow 7a_1$	R
4^2B_2	7.54		8.7(−3)	$3b_2 \rightarrow 4b_2$	R
5^2B_2	7.80		5.3(−3)	$6a_1 \rightarrow 8a_1$	R
6^2B_2	7.81		2.7(−4)	$1b_1 \rightarrow 2b_1$	V
7^2B_2	8.74		1.3(−3)	$6a_1 \rightarrow 7a_1$	R
8^2B_2	8.89		5.6(−3)	$3b_2 \rightarrow 5b_2$	R
9^2B_2	9.43		1.5(−3)	$6a_1 \rightarrow 8a_1$	R
1^2A_1	1.22	1.22	1.7(−2)	$6a_1 \rightarrow 3b_2$	V
2^2A_1	5.06	5.17	3.1(−2)	$5a_1 \rightarrow 3b_2$	V
3^2A_1	6.76		1.9(−5)	$3b_2 \rightarrow 7a_1$	R
4^2A_1	7.37		9.3(−3)	$3b_2 \rightarrow 8a_1$	R
5^2A_1	8.46		3.7(−3)	$3b_2 \rightarrow 9a_1$	R
6^2A_1	8.73		8.0(−3)	$1b_1 \rightarrow 2a_2$	V
7^2A_1	8.82		4.9(−3)	$3b_2 \rightarrow 10a_1$	R
8^2A_1	9.14		1.1(−5)	$6a_1 1b_1 \rightarrow 4b_1 3b_2$	V
9^2A_1	9.97		6.9(−4)	$(6a_1)^2 \rightarrow 7a_1 3b_2$	R
1^2A_2	3.90	3.94	2.2(−3)	$3b_2 \rightarrow 2a_2$	V
2^2A_2	4.61	4.94	1.8(−2)	$6a_1 \rightarrow 2b_1$	V
3^2A_2	5.53		4.2(−4)	$6a_1 \rightarrow 3b_1$	V
4^2A_2	7.50		2.7(−2)	$(6a_1)^2 \rightarrow 3b_2 2a_2$	R
5^2A_2	7.54		1.8(−2)	$6a_1 \rightarrow 4b_1$	R
6^2A_2	8.53		1.3(−2)	$5a_1 \rightarrow 2b_1$	R
7^2A_2	8.72		9.6(−3)	$3b_2 \rightarrow 1a_2$	R
8^2A_2	8.99		7.3(−3)	$6a_1 \rightarrow 3b_1$	R
9^2A_2	9.46		4.0(−3)	$6a_1 \rightarrow 4b_1$	R
1^2B_1	3.47	3.49		$3b_2 \rightarrow 2b_1$	V
2^2B_1	4.70	4.63		$3b_2 \rightarrow 3b_1$	V
3^2B_1	5.73			$6a_1 \rightarrow 1a_2$	V
4^2B_1	5.97			$6a_1 \rightarrow 2a_2$	V
5^2B_1	7.19			$(6a_1)^2 \rightarrow 2b_1 3b_2$	V
6^2B_1	7.51			$3b_2 \rightarrow 4b_1$	R
7^2B_1	8.80			$3b_2 \rightarrow 2b_1$	R
8^2B_1	8.97			$6a_1 \rightarrow 1a_2$	R
9^2B_1	9.09			$5a_1 \rightarrow 2a_2$	R

[a] Ground state energy including Davidson correction: −114.393014 hartree.

Table 5
Vertical excitation energies, oscillator strengths and dominant configurations for HC_3H at the ground state equilibrium geometry

State	Energy (eV) This work	f^{el} This work	Dominant configuration	Type
1^3B[a]	0.00	⋯	$\cdots 6a^2 7a^1 3b^2 4b^1$	V
2^3B	4.37	1.8(−4)	$3b \rightarrow 4b$	V
3^3B	4.58	1.2(−5)	$6a \rightarrow 7a$	V
4^3B	5.61	4.2(−5)	$7a \rightarrow 9a$	R
5^3B	5.89	7.5(−4)	$7a \rightarrow 8a$	V
6^3B	6.08	6.7(−4)	$4b \rightarrow 5b$	V
7^3B	6.67	7.0(−6)	$7a \rightarrow 10a$	R
8^3B	6.93	6.8(−4)	$4b \rightarrow 6b$	R
9^3B	6.97	1.9(−4)	$7a \rightarrow 11a$	R
1^3A	4.23	1.7(−2)	$7a \rightarrow 4b$	V
2^3A	4.33	2.4(−4)	$3b \rightarrow 7a$	V
3^3A	5.66	9.3(−4)	$4b \rightarrow 8a$	V
4^3A	5.97	1.7(−3)	$7a \rightarrow 5b$	V
5^3A	6.29	1.5(−1)	$7a \rightarrow 6b$	R
6^3A	6.68	1.2(−3)	$4b \rightarrow 9a$	R
7^3A	6.95	4.8(−3)	$4b \rightarrow 10a$	R
8^3A	7.52	2.4(−1)	$4b \rightarrow 12a$	R
9^3A	7.73	2.2(−3)	$4b \rightarrow 13a$	R

[a] Ground state energy including Davidson correction: −114.924751 hartree.

The equilibrium structures of the electronic ground states are taken from Seburg et al., their Fig. 5 [54]. Our calculated relative ordering of the C_3H_2 isomers is consistent with previous findings but due to different amounts of recovered correlation energy, our energy splittings are larger than in other studies.

The adiabatic ionization potentials of the various C_3H_2 isomers lie at 8.96 (HC_3H), 9.2 (c-C_3H_2) and 10.4 eV (l-C_3H_2), respectively (Table 11). Above these thresholds, the photoionization efficiency of all three C_3H_2 isomers increases rapidly so that photoionization will become the main pathway [58]. Some of these ionizations are likely to be dissociative, but this option is not considered here.

3.4.1. HC_3H

The HC_3H radical has C_2 geometry with a ^3B ground state. In this case, the C_2 axis was put through the middle C atom and the middle of the H1–H2 line. Table 5 summarizes our computed vertical excitation energies, oscillator strengths and configurations. For the lowest four excited states, our results are in good agreement with those of Mebel et al. [59] (their MRCI + D(4,8)/ANO(2+) results). The dissociation energy of HC_3H to l-C_3H + H is computed to be around 3.1 eV, with the dissociation energy to $C_3 + H_2$ perhaps even less [59]. Of the dipole-allowed states above the dissociation and below the ionization limit at 8.96 eV, the higher ^3A states at 6.2 and 7.5 eV, both of which have $\pi \rightarrow \pi^*$ character, have the largest oscillator strengths.

3.4.2. c-C_3H_2

The c-C_3H_2 molecule has a $^1A_1$ ground state in its C_{2v} geometry, with a large dipole moment of 3.4 Debye owing to the two unpaired electrons on one of the three carbon atoms. Table 6 summarizes our computed vertical excitation energies and oscillator strengths, which again agree well in terms of energies with those of Mebel et al. [59], although our oscillator strengths are somewhat lower. Compared with c-C_3H, c-C_3H_2 has only few low-lying electronic states, and all of the dipole-allowed transitions lie above the dissociation energy of 4.4 eV [59]. Those to the 6^1A_1 ($\pi \rightarrow \pi^*$) at 9.4, 7^1B_1 at 10.6 and 9^1B_1 state at 11.2 eV have the largest oscillator strengths. However, none of these states lie below the ionization potential of c-C_3H_2 at 9.2 eV. Thus, its photodissociation rate will differ substantially whether or not these states are included (see Section 4).

3.4.3. l-C_3H_2

The vinylidenecarbene or propadienylidene isomer of C_3H_2, denoted here as l-C_3H_2, also has $^1A_1$ symmetry in

Table 6
Vertical excitation energies, oscillator strengths and dominant configurations for c-C_3H_2 at the ground state equilibrium geometry

State	Energy (eV) This work	f^{el} This work	Dominant configuration	Type
1^1A_1[a]	0.00	···	$\cdots 5a_1^2 6a_1^2 1b_1^2 2b_2^2 3b_2^2$	V
2^1A_1	6.31	1.1(−4)	$6a_1 \rightarrow 8a_1$	R
3^1A_1	6.85	6.7(−2)	$6a_1 \rightarrow 9a_1$	R
4^1A_1	7.82	1.1(−2)	$6a_1 \rightarrow 10a_1$	R
5^1A_1	8.11	2.9(−3)	$6a_1 \rightarrow 9a_1$	R
6^1A_1	8.57	7.0(−2)	$6a_1 \rightarrow 11a_1$	R
7^1A_1	9.37	1.2(−1)	$1b_1 \rightarrow 2b_1$	V
8^1A_1	9.70	4.8(−2)	$6a_1 \rightarrow 12a_1$	R
9^1A_1	10.94	8.7(−4)	$6a_1 \rightarrow 12a_1$	R
1^1B_1	4.89	2.8(−2)	$6a_1 \rightarrow 5b_1$	V
2^1B_1	6.65	2.4(−3)	$3b_2 \rightarrow 1a_2$	V
3^1B_1	6.91	1.9(−2)	$6a_1 \rightarrow 2b_1$	R
4^1B_1	8.25	6.3(−3)	$6a_1 \rightarrow 3b_1$	R
5^1B_1	8.63	1.1(−2)	$1b_1 \rightarrow 8a_1$	R
6^1B_1	10.30	4.3(−2)	$1b_1 \rightarrow 9a_1$	R
7^1B_1	11.16	2.6(−2)	$3b_2 \rightarrow 1a_2$	R
8^1B_1	11.53	1.8(−4)	$1b_1 \rightarrow 10a_1$	R
9^1B_1	12.30	1.3(−3)	$6a_1 \rightarrow 4b_1$	R
1^1B_2	6.68	1.4(−4)	$6a_1 \rightarrow 6b_2$	R
2^1B_2	8.13	4.4(−3)	$6a_1 \rightarrow 7b_2$	R
3^1B_2	8.29	1.1(−2)	$6a_1 \rightarrow 4b_2$	V
4^1B_2	9.01	6.6(−2)	$1b_1 \rightarrow 1a_2$	R
5^1B_2	9.20	5.8(−3)	$3b_2 \rightarrow 8a_1$	R
6^1B_2	9.99	3.0(−2)	$3b_2 \rightarrow 9a_1$	R
7^1B_2	10.58	3.0(−1)	$6a_1 \rightarrow 5b_2$	V
8^1B_2	11.03	1.6(−5)	$3b_2 \rightarrow 8a_1$	R
9^1B_2	11.23	1.0(−1)	$6a_1 \rightarrow 8b_2$	R
1^1A_2	3.92		$6a_1 \rightarrow 1a_2$	V
2^1A_2	7.03		$3b_2 \rightarrow 5b_1$	V
3^1A_2	8.46		$6a_1 \rightarrow 2a_2$	R
4^1A_2	9.25		$5a_1 \rightarrow 2a_2$	V
5^1A_2	9.94		$3b_2 \rightarrow 2b_1$	R
6^1A_2	10.86		$1b_1 \rightarrow 4b_2$	R
7^1A_2	11.28		$2b_2 \rightarrow 3b_1$	R
8^1A_2	12.31		$1b_1 \rightarrow 4b_2$	R
9^1A_2	12.65		$2b_2 \rightarrow 3b_1$	R

[a] Ground state energy including Davidson correction: −115.037418 hartree.

Table 7
Vertical excitation energies, oscillator strengths and dominant configurations for l-C_3H_2 at the ground state equilibrium geometry

State	Energy (eV) This work	f^{el} This work	Dominant configuration	Type
1^1A_1[a]	0.00	···	$\cdots 6a_1^2 7a_1^2 1b_1^2 2b_2^2$	V
2^1A_1	5.54	1.3(−1)	$1b_1 \rightarrow 2b_1$	V
3^1A_1	5.98	4.7(−2)	$(2b_2)^2 \rightarrow (2b_1)^2$	V
4^1A_1	7.79	9.8(−2)	$2b_2 \rightarrow 3b_2$	R
5^1A_1	8.87	1.5(−2)	$2b_2 \rightarrow 4b_2$	R
6^1A_1	9.00	3.0(−1)	$2b_2 \rightarrow 5b_2$	R
7^1A_1	9.38	3.0(−1)	$2b_2 \rightarrow 6b_2$	R
8^1A_1	9.84	8.8(−2)	$2b_2 \rightarrow 7b_2$	R
9^1A_1	10.02	6.2(−2)	$1b_1 \rightarrow 3b_1$	R
1^1B_1	2.44	8.8(−3)	$7a_1 \rightarrow 2b_1$	V
2^1B_1	6.36	1.3(−2)	$7a_1 1b_1 \rightarrow (2b_1)^2$	V
3^1B_1	8.01	1.7(−2)	$7a_1 \rightarrow 3b_1$	R
4^1B_1	8.82	1.3(−3)	$7a_1 2b_2 \rightarrow 2b_1 5b_2$	V
5^1B_1	8.86	3.8(−3)	$7a_1 \rightarrow 4b_1$	R
6^1B_1	8.88	7.9(−2)	$1b_1 \rightarrow 10a_1$	R
7^1B_1	9.11	2.1(−2)	$7a_1 \rightarrow 5b_1$	R
8^1B_1	9.85	3.6(−3)	$7a_1 \rightarrow 6b_1$	R
9^1B_1	10.13	1.9(−2)	$1b_1 \rightarrow 8a_1$	R
1^1B_2	6.06	2.4(−4)	$6a_1 2b_2 \rightarrow (2b_1)^2$	V
2^1B_2	6.92	1.3(−2)	$2b_2 \rightarrow 8a_1$	V
3^1B_2	8.07	4.0(−2)	$2b_2 \rightarrow 9a_1$	R
4^1B_2	8.87	4.2(−4)	$2b_2 \rightarrow 10a_1$	R
5^1B_2	8.98	2.0(−4)	$2b_2 \rightarrow 11a_1$	R
6^1B_2	9.36	1.9(−2)	$2b_2 \rightarrow 12a_1$	R
7^1B_2	9.68	7.2(−5)	$2b_2 \rightarrow 13a_1$	R
8^1B_2	10.14	3.4(−2)	$2b_2 \rightarrow 14a_1$	R
9^1B_2	10.50	<1(−6)	$2b_2 \rightarrow 15a_1$	R
1^1A_2	1.86		$2b_2 \rightarrow 2b_1$	V
2^1A_2	6.68		$1b_1 2b_2 \rightarrow (2b_1)^2$	V
3^1A_2	7.71		$2b_2 \rightarrow 3b_1$	R
4^1A_2	8.30		$2b_2 \rightarrow 4b_1$	V
5^1A_2	8.86		$2b_2 \rightarrow 5b_1$	R
6^1A_2	8.88		$1b_1 \rightarrow 3b_2$	V
7^1A_2	9.00		$2b_2 \rightarrow 6b_1$	R
8^1A_2	9.17		$2b_2 \rightarrow 7b_1$	R
9^1A_2	9.91		$2b_2 \rightarrow 8b_1$	R

[a] Ground state energy including Davidson correction: −114.965558 hartree.

its C_{2v} ground state geometry. Our computed vertical excitation energies (Table 7) of 1.86, 2.44 and 5.54 eV to the $\widetilde{A}^1A_2$, $\widetilde{B}^1B_1$ and $\widetilde{C}(2)^1A_1$ states are consistent with the experimental adiabatic values [60] of 1.73, 2.00 and 4.84 eV, respectively, and agree within 0.1–0.2 eV with the vertical values computed by Mebel et al. [59]. The dissociation energy of l-C_3H_2 to $C_3H + H$ is computed to lie around 3.9 eV, so that only the $\widetilde{C}(2)^1A_1$ and higher states can lead to photodissociation. The $\widetilde{C}$ state shows a well-resolved progression in its electronic spectrum [60], but the resolution of those data is not high enough to measure predissociation rates. Thus, we consider the photodissociation both with and without taking the $\widetilde{C}$ state into account.

Of the dipole-allowed transitions below the ionization potential at 10.4 eV, those to the higher $^1A_1$ states around 9 eV have the strongest oscillator strengths. These states all have $2b_2 \rightarrow n^*b_2$ character and likely belong to the Rydberg series converging to the lowest ionization potential. Similarly, the higher $^1B_2$ states belong to the $2b_2 \rightarrow na_1$ Rydberg series.

3.5. C_4

The lowest energy $X^3\Sigma_g^-$ ground state of C_4 occurs for the linear geometry. C_4 has been searched for in diffuse interstellar clouds through its $^3\Sigma_u^- \leftarrow {}^3\Sigma_g^-$ transition around 3789 Å but not yet detected [61]. However, a pattern of bands at 57 μm observed with the *Infrared Space Observatory* toward a handful of objects [62] is consistent with transitions in the ν_5 bending mode [63]. Rhombic C_4, which is almost isoenergetic with l-C_4, has not yet been detected in interstellar space.

Our calculations use the l-C_4 equilibrium values computed by Botschwina [64], which are consistent with experiments [23]. The results are presented in Table 8. Our excitation energies of the lower states are in good

Table 8
Vertical excitation energies and oscillator strengths and dominant configurations for l-C_4 at the ground state equilibrium geometry

State	Energy (eV)			f^{el}	Dominant configuration	Type
	This work	Ref. [65]	Exp. [65]	This work		
$1^3\Sigma_g^-$[a]	0.00	0.00	0.00	···	$\cdots 4\sigma_u^2 5\sigma_g^2 1\pi_u^4 1\pi_g^2$	V
$2^3\Sigma_g^-$	6.40	6.11			$\cdots 4\sigma_u^2 5\sigma_g^2 1\pi_u^3 1\pi_g^3$	V
$3^3\Sigma_g^-$	6.79				$\cdots 4\sigma_u^2 5\sigma_g^2 1\pi_u^3 1\pi_g^2 2\pi_u^1$	V
$4^3\Sigma_g^-$	7.05				$\cdots 4\sigma_u^2 5\sigma_g^2 1\pi_u^3 1\pi_g^2 2\pi_u^1$	V
$1^3\Sigma_g^+$	5.80				$\cdots 4\sigma_u^1 5\sigma_g^1 1\pi_u^4 1\pi_g^3 2\pi_u^1$	V
$1^3\Sigma_u^-$	3.61	3.74	3.27	9.4(−03)	$\cdots 4\sigma_u^2 5\sigma_g^2 1\pi_u^3 1\pi_g^3$	V
$2^3\Sigma_u^-$	6.95			1.6(+0)	$\cdots 4\sigma_u^2 5\sigma_g^2 1\pi_u^4 1\pi_g^1 2\pi_u^1$	V
$1^3\Sigma_u^+$	1.68				$\cdots 4\sigma_u^1 5\sigma_g^1 1\pi_u^4 1\pi_g^4$	V
$2^3\Sigma_u^+$	2.82	2.84			$\cdots 4\sigma_u^2 5\sigma_g^2 1\pi_u^3 1\pi_g^3$	V
$3^3\Sigma_u^+$	4.30				$\cdots 4\sigma_u^2 5\sigma_g^2 1\pi_u^4 1\pi_g^1 2\pi_u^1$	V
$4^3\Sigma_u^+$	4.65				$\cdots 4\sigma_u^2 1\pi_u^4 1\pi_g^3 2\pi_u^1$	V
$5^3\Sigma_u^+$	5.63				$\cdots 5\sigma_g^2 1\pi_u^4 1\pi_g^3 2\pi_u^1$	V
$1^3\Pi_g$	0.95	1.09	0.82		$\cdots 4\sigma_u^2 5\sigma_g^1 1\pi_u^4 1\pi_g^3$	V
$2^3\Pi_g$	4.26				$\cdots 4\sigma_u^1 5\sigma_g^2 1\pi_u^3 1\pi_g^4$	V
$3^3\Pi_g$	5.31				$\cdots 4\sigma_u^1 5\sigma_g^2 1\pi_u^4 1\pi_g^2 2\pi_u^1$	V
$4^3\Pi_g$	5.96				$\cdots 4\sigma_u^1 5\sigma_g^2 1\pi_u^4 1\pi_g^2 2\pi_u^1$	V
$1^3\Pi_u$	1.19	1.37	0.93	4.6(−3)	$\cdots 4\sigma_u^1 5\sigma_g^2 1\pi_u^4 1\pi_g^3$	V
$2^3\Pi_u$	4.00			2.2(−4)	$\cdots 4\sigma_u^2 5\sigma_g^1 1\pi_u^3 1\pi_g^4$	V
$3^3\Pi_u$	5.10			1.6(−2)	$\cdots 4\sigma_u^2 5\sigma_g^1 1\pi_u^4 1\pi_g^2 2\pi_u^1$	V
$4^3\Pi_u$	5.70			2.8(−5)	$\cdots 4\sigma_u^2 5\sigma_g^1 1\pi_u^4 1\pi_g^2 2\pi_u^1$	V
$5^3\Pi_u$	5.86			1.2(−1)	$\cdots 4\sigma_u^2 5\sigma_g^1 1\pi_u^4 1\pi_g^2 2\pi_u^1$	V
$1^3\Delta_u$	2.77	2.82			$\cdots 4\sigma_u^2 5\sigma_g^2 1\pi_u^3 1\pi_g^3$	V
$2^3\Delta_u$	4.25	3.56			$\cdots 4\sigma_u^2 5\sigma_g^2 1\pi_u^4 1\pi_g^1 2\pi_u^1$	V
$1^3\Delta_g$	6.67				$\cdots 4\sigma_u^2 5\sigma_g^2 1\pi_u^3 1\pi_g^2 2\pi_u^1$	V

[a] Ground state energy including Davidson correction: −152.228684 hartree.

agreement with experiments and with the calculations of Massó et al. [65], except for the $2^3\Delta_u$ state. Note that the experimental values refer to T_0 rather than T_e, which can differ by a few tenths of eV. Our computed dissociation energy D_e is 4.7 eV, in good agreement with the experimentally inferred D_0 value of 4.71 ± 0.15 eV [66].

The lowest excited state above the dissociation limit to which dipole-allowed transitions are possible is the $3^3\Pi_u$ state at 5.1 eV. Indeed, photofragment yield spectra in the 2.22–5.40 eV range by Choi et al. [66] show significant single-photon dissociation into $C_3 + C$ at $\geqslant$5.2 eV, with a minor channel to $C_2 + C_2$. Their spectra are well reproduced by phase space theory models in which the product state distributions are statistical. This implies that absorption into the excited state is most likely followed by rapid internal conversion to the ground state potential energy surface with no barriers present along the dissociation coordinates.

By far the strongest absorption occurs into the $2^3\Sigma_u^-$ state around 6.95 eV, which has an oscillator strength of 1.56. Even though higher Σ_u^- and Π_u states will contribute, the $2^3\Sigma_u^-$ channel will dominate the interstellar photodissociation of C_4, if indeed every absorption is followed by dissociation.

3.6. l-C_4H

The l-C_4H (butadiynyl) radical was detected in the envelopes of carbon-rich evolved stars nearly 30 years ago [67]. It was subsequently found to be very abundant in cold dark clouds like TMC-1 [68] and even detected in comets [17]. It is one of the carbon-bearing molecules found at the edges of PDRs [15], where it can photodissociate into smaller species.

C_4H has linear symmetry with a $^2\Sigma^+$ ground state. The equilibrium coordinates in our calculations were taken from Ref. [69]. Table 9 summarizes our computed vertical excitation energies, oscillator strengths and configurations. Comparison with the results of Graf et al. [70] shows good agreement in both energies and transition dipole moments for the lowest states, but poor agreement for the higher $^2\Pi$ states, where the Graf et al. energies are generally lower by up to 1 eV. There are two main reasons for this. First, Graf et al. did not include diffuse (Rydberg) functions in their basis set, which start to become important for the higher states. Second, their CASPT2 perturbation method does not guarantee a lower bound to the energies. Our calculations agree in the fact that none of the higher-lying $^2\Pi$ states have large oscillator strengths.

The threshold for photodissociation, corresponding to dissociation of C_4H to $C_4 + H$, lies around 4.7 eV (Table 11). Of the dipole-allowed transitions below the ionization potential at 9.6 eV, the 4 and $5^2\Sigma^+$ states at 7.7 and 8.7 eV, respectively, have orders of magnitude larger oscillator strengths than other states and will thus dominate the

Table 9
Vertical excitation energies,oscillator strengths and dominant configurations for l-C_4H at the ground state equilibrium geometry

State	Energy (eV)		f^{el}		Dominant configuration	Type
	This work	Ref. [70]	This work	Ref. [70]		
$1^2\Sigma^+$[a]	0.00	0.00	···	···	$\cdots 9\sigma^1 1\pi^4 2\pi^4$	V
$2^2\Sigma^+$	5.11	4.76	1.0(−6)	<7(−7)	$\cdots 9\sigma^1 1\pi^4 2\pi^3 3\pi^1$	V
$3^2\Sigma^+$	7.36	6.62	9.5(−4)	1.8(−3)	$\cdots 9\sigma^1 1\pi^3 2\pi^4 3\pi^1$	V
$4^2\Sigma^+$	7.74		3.5(−1)		$\cdots 9\sigma^1 1\pi^4 3\pi^3 3p_\pi^1$	R
$5^2\Sigma^+$	8.76		5.5(−1)		$\cdots 9\sigma^1 1\pi^4 2\pi^3 3p_\pi^1$	R
$1^2\Pi$	0.37	0.44	7.8(−4)	8.4(−4)	$\cdots 9\sigma^2 1\pi^4 2\pi^3$	V
$2^2\Pi$	3.59	3.31	7.8(−4)	9.8(−4)	$\cdots 9\sigma^2 1\pi^3 2\pi^4$	V
$3^2\Pi$	5.31	4.71	3.4(−4)	7.2(−4)	$\cdots 9\sigma^2 1\pi^4 2\pi^3 3\pi^1$	V
$4^2\Pi$	7.15	5.92	2.2(−3)	9.2(−4)	$\cdots 9\sigma^1 10\sigma^1 1\pi^4 2\pi^3$	R
$5^2\Pi$	7.85	6.82	7.0(−3)	8.8(−5)	$\cdots 9\sigma^1 10\sigma^1 1\pi^4 2\pi^3$	R
$6^2\Pi$	7.90	7.84	1.4(−2)		$\cdots 9\sigma^1 10\sigma^1 1\pi^4 2\pi^3$	R
$7^2\Pi$	8.41		2.2(−3)		$\cdots 9\sigma^1 11\sigma^1 1\pi^4 2\pi^3$	R
$1^2\Sigma^-$	6.03				$\cdots 9\sigma^1 1\pi^4 2\pi^3 3\pi^1$	V
$2^2\Sigma^-$	6.48				$\cdots 9\sigma^1 1\pi^4 2\pi^3 3\pi^1$	V
$3^2\Sigma^-$	8.58				$\cdots 9\sigma^1 1\pi^4 2\pi^3 3p_\pi^1$	R
$4^2\Sigma^-$	8.86				$\cdots 9\sigma^1 1\pi^4 2\pi^3 3p_\pi^1$	R
$1^2\Delta$	5.76	5.20			$\cdots 9\sigma^1 1\pi^4 2\pi^3 3\pi^1$	V
$2^2\Delta$	5.97	5.21			$\cdots 9\sigma^1 1\pi^4 2\pi^3 3\pi^1$	V
$3^2\Delta$	7.85				$\cdots 9\sigma^1 1\pi^3 2\pi^3 3p_\pi^1$	R
$4^2\Delta$	8.10				$\cdots 9\sigma^1 1\pi^3 2\pi^3 3p_\pi^1$	R

[a] Ground state energy including Davidson correction: −152.228684 hartree.

photodissociation. Both states have $1\pi \rightarrow n\pi$ Rydberg character. Thus, our overall photodissociation rate will be significantly larger than that using the data from Graf et al. [70].

3.7. *l*-C_5H

Like C_4H, *l*-C_5H is detected toward the carbon-rich evolved star IRC + 10216 [71] and in cold dark clouds [72]. It also has linear symmetry but with a $^2\Pi$ ground state. The equilibrium coordinates in our calculations were taken from Ref. [69]. Table 10 summarizes our results. Comparison with Haubrich et al. [73] shows excellent agreement in both energies and oscillator strengths, except for the higher-lying $^2\Sigma^+$ states. This difference is likely due to the explicit inclusion of Rydberg states in our work. For the 3 and $4^2\Pi$ states, the oscillator strengths differ by a factor of 2 but these states show considerable interaction between the $2\pi \rightarrow 3\pi$ and $3\pi \rightarrow 4\pi$ ($\pi \rightarrow \pi^*$) excitations. Differences in mixing ratios can lead to large changes in transition dipole moments to individual states, but not in energies. The computed excitation energies for the lowest two excited states also agree well with those measured and computed by Ding et al. [74].

The threshold for photodissociation lies around 3.6 eV (Table 11). Of the dipole-allowed transitions below the ionization potential at 7.4 eV, both the $4^2\Pi$ ($2\pi \rightarrow 3\pi$) state at 4.2 eV and the $6^2\Pi$ ($1\pi \rightarrow 3\pi$) state around 6.1 eV have large oscillator strengths. All other states have typical oscillator strengths of a few $\times 10^{-3}$ and thus contribute at a lower level.

Table 10
Vertical excitation energies, oscillator strengths and dominant configurations for *l*-C_5H at the ground state equilibrium geometry

State	Energy (eV)		f^{el}		Dominant configuration	Type
	This work	Ref. [73][b]	This work	Ref. [73][b]		
$1^2\Pi$[a]	0.00	0.00	⋯	⋯	$\cdots 11\sigma^2 1\pi^4 2\pi^4 3\pi^1$	V
$2^2\Pi$	3.05	3.21	5.1(−4)	1(−3)	$\cdots 11\sigma^2 1\pi^4 2\pi^3 3\pi^2$	V
$3^2\Pi$	3.91	3.99	1.8(−3)	4(−3)	$\cdots 11\sigma^2 1\pi^4 2\pi^3 3\pi^2$	V
$4^2\Pi$	4.18	4.19	5.7(−2)	3(−2)	$\cdots 11\sigma^2 1\pi^4 2\pi^3 3\pi^2$	V
$5^2\Pi$	5.20	5.10	3.5(−3)	5(−3)	$\cdots 11\sigma^2 1\pi^3 2\pi^4 3\pi^2$	V
$6^2\Pi$	6.09	6.35	5.2(−2)	1(−3)	$\cdots 11\sigma^2 1\pi^3 2\pi^4 3\pi^2$	V
$7^2\Pi$	6.13	6.11	3.0(−3)	1.4(−1)	$\cdots 11\sigma^2 1\pi^3 2\pi^4 3\pi^2$	V
$1^2\Sigma^+$	3.21	3.19	4.6(−3)	9(−3)	$\cdots 11\sigma^1 1\pi^4 2\pi^4 3\pi^2$	V
$2^2\Sigma^+$	5.07	6.28	3.4(−3)	1(−3)	$\cdots 11\sigma^2 1\pi^4 2\pi^4 3s^1$	R
$3^2\Sigma^+$	5.73	7.01	1.0(−6)	2(−3)	$\cdots 11\sigma^2 1\pi^4 2\pi^4 3p^1_\sigma$	R
$4^2\Sigma^+$	6.69		1.9(−3)		$\cdots 11\sigma^2 1\pi^4 2\pi^4 4s^1$	R
$5^2\Sigma^+$	7.09		2.0(−6)		$\cdots 11\sigma^2 1\pi^3 2\pi^3 3\pi^2$	V
$1^2\Sigma^-$	2.83	2.80	6.0(−3)	7(−3)	$\cdots 11\sigma^1 1\pi^4 2\pi^4 3\pi^2$	V
$2^2\Sigma^-$	5.12	5.25	1.6(−3)	1(−3)	$\cdots 11\sigma^1 1\pi^4 2\pi^3 3\pi^3$	V
$3^2\Sigma^-$	5.99	6.22	2.6(−3)	1(−3)	$\cdots 11\sigma^1 1\pi^4 2\pi^3 3\pi^3$	V
$1^2\Delta$	2.71	2.62	4.8(−3)	3(−3)	$\cdots 11\sigma^1 1\pi^4 2\pi^4 3\pi^2$	V
$2^2\Delta$	6.06	5.92	2.6(−3)	1(−3)	$\cdots 11\sigma^1 1\pi^4 2\pi^3 3\pi^3$	V
$3^2\Delta$	6.63	6.05	1.5(−3)	2(−3)	$\cdots 11\sigma^2 12\sigma^1 1\pi^4 2\pi^4$	V

[a] Ground state energy including Davidson correction: −189.983327 hartree.
[b] Their cc-p-VTZ + SP triple ζ results if available, double ζ results otherwise.

Table 11
Dissociation and ionization energies[a] with respect to ground-state equilibrium energy (in eV) for various species

Species	Products	ΔE_{diss}	Ref.	ΔE_{ion}	Ref.
l-C_3	$C_2 + C(^3P)$	4.63	[75]	12.1	[76]
l-C_4	$C_3 + C(^3P)$	4.71	[66]	10.7	[77]
l-C_2H	$C_2 + H$	4.90	TW[b]	11.4	TW
l-C_3H	$C_3 + H$	3.27	TW	8.6	TW
c-C_3H	$C_3 + H$	4.29	TW	9.6	TW
l-C_4H	$C_4 + H$	4.65	TW	9.6	TW
l-C_5H	$C_5 + H$	3.56	TW	7.4	TW
HC_3H	$C_3H + H$	3.1	[59]	8.96	[58]
c-C_3H_2	$C_3H + H$	4.37	[59]	9.15	[78]
l-C_3H_2	$C_3H + H$	3.87	[59]	10.43	[78]

[a] Experimental data refer to the adiabatic ionization potentials; computed values in this work to vertical ionization potentials.
[b] Computed in this work, using the same basis set and procedure for the products; dissociation energies were obtained at 20 Bohr.

4. Interstellar photodissociation rates

In Table 12, the computed photodissociation rates in the unshielded interstellar radiation field cf. Draine [30] are presented, using the oscillator strengths given in Tables 1–10 and assuming $\eta_u = 1$ for all states. Thus, these rates should be regarded as upper limits. Only states above the dissociation limit and below the ionization potential have been taken into account (see Table 11 for adopted values). No corrections have been made for possible higher-lying states below the ionization limit not computed in this work. Since the oscillator strengths for Rydberg states decrease roughly as $1/n^3$, it is assumed that any such corrections would be small since the lowest Rydberg members are calculated explicitly. For reference, inclusion of a hypothetical state at 9 eV with an oscillator strength of 0.1 would increase the photodissociation rates by only 3.5×10^{-10} s^{-1}.

For C_2H, our new rate is a factor of 3 larger than that given in van Dishoeck et al. [34], which was based on the energies and oscillator strengths of Shih et al. [24]. The increase is mostly due to the higher $^2\Sigma^+$ and $^2\Pi$ states which were not computed in that work. For C_3, the new rate is only 30% larger, mostly because the photodissociation rate of this molecule is dominated by the very strong

Table 12
Photodissociation rates (in s^{-1}) for various molecules in the unshielded interstellar radiation field

Species	Rate
l-C_3	5.0(−9)
l-C_4	8.5(−9)
l-C_2H	1.6(−9)
l-C_3H	1.8(−9)
c-C_3H	1.1(−9)
l-C_4H	3.7(−9)
l-C_5H	1.3(−9)
HC_3H	2.2(−9)
c-C_3H_2	1.4(−9)
l-C_3H_2	5.1(−9)

absorption into the $1^1\Sigma_u^+$ state around 8 eV, which was included in previous estimates.

It is seen that the rates for the various carbon-bearing molecules span a range of a factor of 8, with the rates for the bare carbon chains (C_3, C_4) being largest and those for the odd-numbered C_nH species lowest. Of the different C_3H_2 isomers, l-C_3H_2 has the largest photodissociation rate and c-C_3H_2 the smallest by a factor of 3. However, c-C_3H_2 differs from the other isomers in that it has several states with large oscillator strengths above the ionization potential of 9.15 eV. If those states were included, the c-C_3H_2 photodissociation rate would be increased by a factor of 2. For l-C_3H_2, the rate would drop from 5.1×10^{-9} to 4.1×10^{-9} s^{-1} if the $\tilde{C}$ state is not included.

In spite of the range of values, all rates are above 10^{-9} s^{-1}, corresponding to a lifetime of less than 30 years at the edge of an interstellar cloud. In regions such as the Orion Bar and the Horsehead nebula, the radiation field is enhanced by factors of 10^3–10^5 compared with the standard field adopted here, decreasing the lifetimes to less than 1 month. Thus, there must be rapid production routes of these molecules in order to explain their high abundances in UV-exposed regions. This conclusion is not changed if only 10%, say, of the absorptions would lead to dissociation rather than the 100% assumed here. As argued in Sections 2 and 3, it is plausible that a substantial fraction of the absorptions lead to dissociation for these larger molecules so that the upper limits should be close to the actual values.

5. Conclusions

We have presented vertical excitation energies, transition dipole moments and oscillator strengths for states up to the 9th root of each symmetry for several carbonaceous molecules of astrophysical interest. For lower-lying states, good agreement is generally found with previous studies. Several new, higher-lying states with large oscillator strengths, often of Rydberg character, are revealed in this work.

The calculated photodissociation rates of the small carbon-bearing molecules studied here are substantial, leading to lifetimes at the edges of interstellar clouds of less than 30 years. These high rates assume that all absorptions above the dissociation limit indeed lead to dissociation, so that the rates should be viewed as upper limits. Further experimental work is needed to quantify the dissociation efficiencies for the strongest states found in this work.

Acknowledgements

Our calculations of the photodissociation processes of astrophysical molecules, which started 30 years ago, were made possible through the Wuppertal–Bonn MRD-CI set of quantum-chemical programs kindly made available by Prof. S.D. Peyerimhoff and Prof. R.J. Buenker. The authors enjoyed many stimulating conversations with Prof. Peyerimhoff on excited electronic states of small molecules over the past decades. Astrochemistry in Leiden is supported by a Spinoza grant from the Netherlands Organization for Scientific Research (NWO).

References

[1] K.D. Tucker, M.L. Kutner, P. Thaddeus, Astrophys. J. 193 (1974) L115.
[2] M.B. Bell, P.A. Feldman, J.K.G. Watson, M.C. McCarthy, M.J. Travers, C.A. Gottlieb, P. Thaddeus, Astrophys. J. 518 (1999) 740.
[3] M.B. Bell, P.A. Feldman, M.J. Travers, M.C. McCarthy, C.A. Gottlieb, P. Thaddeus, Astrophys. J. 483 (1997) L61.
[4] P. Thaddeus, J.M. Vrtilek, C.A. Gottlieb, Astrophys. J. 299 (1985) L63.
[5] M.C. McCarthy, C.A. Gottlieb, H. Gupta, P. Thaddeus, Astrophys. J. 652 (2006) L141.
[6] L. Hobbs, Astrophys. J. 232 (1979) L175.
[7] E.F. van Dishoeck, P.T. de Zeeuw, Mon. Not. R. Astr. Soc. 206 (1984) 383.
[8] J.P. Maier, N.M. Lakin, G.A.H. Walker, D.A. Bohlender, Astrophys. J. 553 (2001) 267.
[9] P. Cox, R. Guesten, C. Henkel, Astron. Astrophys. 206 (1988) 108.
[10] G. Winnewisser, E. Herbst, Rep. Prog. Phys. 56 (1993) 1209.
[11] E. Herbst, in: V. Pirronello, J. Krelowski, G. Manico (Eds.), Solid State Astrochemistry, Kluwer Academic Publishers, Dordrecht, 2003, p. 105.
[12] D.J. Hollenbach, A.G.G.M. Tielens, Ann. Rev. Astr. Astrophys. 35 (1997) 179.
[13] M.R. Hogerheijde, D.J. Jansen, E.F. van Dishoeck, Astron. Astrophys. 294 (1995) 792.
[14] D. Teyssier, D. Fossé, M. Gerin, J. Pety, A. Abergel, E. Roueff, Astron. Astrophys. 417 (2004) 135.
[15] J. Pety, D. Teyssier, D. Fossé, M. Gerin, E. Roueff, A. Abergel, E. Habart, J. Cernicharo, Astron. Astrophys. 435 (2005) 885.
[16] M. Guélin, R. Lucas, R. Neri, M. Bremer, D. Broguière, in: Y.C. Minh, E.F. van Dishoeck (Eds.), Astrochemistry: From Molecular Clouds to Planetary Systems, IAU Symposium-197, Astronomical Society of the Pacific, San Francisco, 2000, p. 365.
[17] J. Geiss, K. Altwegg, H. Balsiger, S. Graf, Space Sci. Rev. 90 (1999) 253.
[18] T.J. Lee, A. Bunge, H.F. Schaefer III, J. Am. Chem. Soc. 107 (1985) 137.
[19] P. Botschwina, P. Sebald, Chem. Phys. Lett. 160 (1989) 485.
[20] V.K. Jonas, M. Böhme, G. Frenking, J. Phys. Chem. 96 (1992) 1640.
[21] Q. Cui, K. Morokuma, J. Chem. Phys. 108 (1998) 626.
[22] S. Carter, N.C. Handy, C. Puzzarini, R. Tarroni, P. Palmieri, Mol. Phys. 98 (2000) 1697.
[23] A. Van Orden, R.J. Saykally, Chem. Rev. 98 (1998) 2313.
[24] S.-K. Shih, S.D. Peyerimhoff, R.J. Buenker, J. Mol. Spectrosc. 64 (1977) 167.
[25] J. Römelt, S.D. Peyerimhoff, R.J. Buenker, Chem. Phys. Lett. 58 (1978) 1.
[26] E.F. van Dishoeck, M.C. van Hemert, A. Dalgarno, J. Chem. Phys. 77 (1982) 3693.
[27] R. van Harrevelt, M.C. van Hemert, J. Chem. Phys. 114 (2001) 9453.
[28] R. Schinke, Photodissociation Dynamics, Cambridge University Press, Cambridge, 1993.
[29] K.P. Kirby, E.F. van Dishoeck, Adv. At. Mol. Phys. 25 (1988) 437.
[30] B.T. Draine, Astrophys. J. Suppl. 36 (1978) 595.
[31] GAMESS-UK is a package of ab initio programs. See: http://www.cfs.dl.ac.uk/gamess-uk/index.shtm M.F. Guest, I.J. Bush, H.J.J. van Dam, P. Sherwood, J.M.H. Thomas, J.H. van Lenthe, R.W. A Havenith, J. Kendrick, Mol. Phys. 103 (6–8) (2005) 719.
[32] T.H. Dunning, J. Chem. Phys. 55 (1971) 716.
[33] G. Hirsch, P.J. Bruna, S.D. Peyerimhoff, R.J. Buenker, Chem. Phys. Lett. 52 (1977) 442.

[34] E.F. van Dishoeck, B. Jonkheid, M.C. van Hemert, Faraday Discuss. 133 (2006) 855. http://www.strw.leidenuniv.nl/~ewine/photo/.
[35] M.N.R. Ahsfold, J.E. Baggott (Eds.), Molecular Photodissociation Dynamics, Royal Society of Chemistry, London, 1987.
[36] S.-K. Shih, S.D. Peyerimhoff, R.J. Buenker, J. Mol. Spectrosc. 74 (1979) 124.
[37] D. Duflot, J.-M. Robbe, J.-P. Flament, J. Chem. Phys. 100 (1994) 1236.
[38] A.G. Koures, L.B. Harding, J. Phys. Chem. 95 (1991) 1035.
[39] M. Peric, R.J. Buenker, S.D. Peyerimhoff, Mol. Phys. 71 (1990) 673.
[40] W. Huggins, Proc. R. Soc. London 33 (1882) 1.
[41] M.L. Haffner, D.M. Meyer, Astrophys. J. 453 (1995) 450.
[42] K.H. Hinkle, J.J. Keady, P.F. Bernath, Science 241 (1988) 1319.
[43] J. Cernicharo, J.R. Goicoechea, E. Caux, Astrophys. J. 534 (2000) L199.
[44] C.F. Chabalowski, R.J. Buenker, S.D. Peyerimhoff, J. Chem. Phys. 84 (1986) 268.
[45] A. Terentyev, R. Scholz, M. Schreiber, G. Seifert, J. Chem. Phys. 121 (2004) 5767.
[46] G. Monninger, M. Förderer, P. Gürtler, S. Kalhofer, S. Petersen, L. Nemes, P.G. Szalay, W. Krätschmer, J. Phys. Chem. A 106 (2002) 5779.
[47] K.S. Pitzer, E. Clementi, J. Am. Chem. Soc. 81 (1959) 4477.
[48] P. Thaddeus, C.A. Gottlieb, Å. Hjalmarson, L.E.B. Johansson, W.M. Irvine, P. Friberg, R. Linke, Astrophys. J. 294 (1985) L49.
[49] S. Yamamoto, S. Saito, M. Ohishi, H. Suzuki, S. Ishikawa, N. Kaifu, A. Murakami, Astrophys. J. 322 (1987) L55.
[50] J. Takahashi, K. Yamashita, J. Chem. Phys. 104 (1996) 6613.
[51] H. Ding, T. Pino, F. Güthe, J.P. Maier, J. Chem. Phys. 115 (2001) 6913.
[52] S. Yamamoto, S. Saito, J. Chem. Phys. 101 (1994) 5484.
[53] H.E. Matthews, W.M. Irvine, Astrophys. J. 298 (1985) L61.
[54] R.A. Seburg, E.V. Patterson, J.F. Stanton, R.J. McMahon, J.Am. Chem. Soc. 119 (1997) 5847.
[55] J. Cernicharo, C.A. Gottlieb, M. Guelin, T.C. Killian, P. Thaddeus, J.M. Vrtilek, Astrophys. J. 368 (1991) L43.
[56] W.J. Hehre, J.A. Pople, W. A Lathan, L. Radom, E. Wasserman, Z.R. Wasserman, J. Am. Chem. Soc. 98 (1976) 4378.
[57] D.J. DeFrees, A.D. McLean, Astrophys. J. 308 (1986) L31.
[58] C.A. Taatjes, S.J. Klippenstein, N. Hansen, J.A. Miller, T.A. Cool, J. Wang, M.E. Law, P.R. Westmoreland, Phys. Chem. Chem. Phys. 7 (2005) 806.
[59] A.M. Mebel, W.M. Jackson, A.H.H. Chang, S.H. Lin, J. Am. Chem. Soc. 120 (1998) 5751.
[60] J.A. Hodges, R.J. McMahon, K.W. Sattelmeyer, J.F. Stanton, Astrophys. J. 544 (2000) 838.
[61] J.P. Maier, G.A.H. Walker, D.A. Bohlender, Astrophys. J. 566 (2002) 332.
[62] J. Cernicharo, J.R. Goicochea, Y. Benilan, Astrophys. J. 580 (2002) L157.
[63] N. Moazzen-Ahmadi, J.J. Thong, A.R.W. McKellar, J. Chem. Phys. 100 (1994) 4033.
[64] P. Botschwina, J. Mol. Spectrosc. 186 (1997) 203.
[65] H. Massó, M.L. Senent, P. Rosmus, M. Hochlaf, J. Chem. Phys. 124 (2006) 234304.
[66] H. Choi, R.T. Bise, A.A. Hoops, D.H. Mordaunt, D.M. Neumark, J. Phys. Chem. A 104 (2000) 2025.
[67] M. Guélin, S. Green, P. Thaddeus, Astrophys. J. 224 (1978) L27.
[68] W.M. Irvine, B. Hoglund, P. Friberg, J. Askne, J. Elldér, Astrophys. J. 248 (1981) L113.
[69] M.C. McCarthy, P. Thaddeus, J. Chem. Phys. 122 (2005) 174308.
[70] S. Graf, J. Geiss, S. Leutwyler, J. Chem. Phys. 114 (2001) 4542.
[71] J. Cernicharo, C. Kahane, J. Gomez-Gonzalez, M. Guélin, Astron. Astrophys. 167 (1986) L5.
[72] J. Cernicharo, M. Guélin, C.M. Walmsley, Astron. Astrophys. 172 (1987) L5.
[73] J. Haubrich, M. Mühlhäuser, S.D. Peyerimhoff, J. Phys. Chem. A 106 (2002) 8201.
[74] H. Ding, T. Pino, F. Güthe, J.P. Maier, J. Chem. Phys. 117 (2002) 8362.
[75] S.G. Kim, Y.H. Lee, P. Nordlander, D. Tománek, Chem. Phys. Lett. 264 (1997) 345.
[76] J. Benedikt, D.J. Eijkman, W. Vandamme, S. Agarwal, M.C.M. van de Sanden, Chem. Phys. Lett. 402 (2005) 37.
[77] J.V. Ortiz, J. Chem. Phys. 99 (1993) 6716.
[78] H. Clauberg, D.W. Minsek, P. Chen, J. Am. Chem. Soc. 114 (1992) 99.